

OAK RIDGE NATIONAL LABORATORY LIBRARY  
  
3 4456 0023708 1

ORNL/TM-5331

*cy 49*

# Theoretical and Experimental Determination of Mechanical Properties of Superconducting Composite Wire

W. H. Gray  
C. T. Sun

OAK RIDGE NATIONAL LABORATORY  
CENTRAL RESEARCH LIBRARY  
DOCUMENT COLLECTION  
**LIBRARY LOAN COPY**  
DO NOT TRANSFER TO ANOTHER PERSON  
If you wish someone else to see this  
document, send in name with document  
and the library will arrange a loan.  
UCN-7969  
(3 3-67)

**OAK RIDGE NATIONAL LABORATORY**  
OPERATED BY UNION CARBIDE CORPORATION FOR THE ENERGY RESEARCH AND DEVELOPMENT ADMINISTRATION

Printed in the United States of America. Available from  
National Technical Information Service  
U.S. Department of Commerce  
5285 Port Royal Road, Springfield, Virginia 22161  
Price: Printed Copy \$4.50; Microfiche \$2.25

This report was prepared as an account of work sponsored by the United States Government. Neither the United States nor the Energy Research and Development Administration/United States Nuclear Regulatory Commission, nor any of their employees, nor any of their contractors, subcontractors, or their employees, makes any warranty, express or implied, or assumes any legal liability or responsibility for the accuracy, completeness or usefulness of any information, apparatus, product or process disclosed, or represents that its use would not infringe privately owned rights.

Contract No. W-7405-eng-26

THEORETICAL AND EXPERIMENTAL DETERMINATION OF MECHANICAL  
PROPERTIES OF SUPERCONDUCTING COMPOSITE WIRE

W. H. Gray  
Superconducting Magnet Development Program  
Thermonuclear Division

and

C. T. Sun  
Iowa State University

JULY 1976

**NOTICE** This document contains information of a preliminary nature  
and was prepared primarily for internal use at the Oak Ridge National  
Laboratory. It is subject to revision or correction and therefore does  
not represent a final report.

OAK RIDGE NATIONAL LABORATORY  
Oak Ridge, Tennessee 37830  
operated by  
UNION CARBIDE CORPORATION  
for the  
ENERGY RESEARCH AND DEVELOPMENT ADMINISTRATION



3 4456 0023708 1



TABLE OF CONTENTS

ABSTRACT . . . . . 1

INTRODUCTION . . . . . 1

THEORETICAL INVESTIGATION . . . . . 2

1.1 Self-Consistent Model Methods . . . . . 2

1.2 Variational Methods . . . . . 3

1.3 Exact Methods . . . . . 3

1.4 Mechanics of Materials Method . . . . . 3

1.5 The Halpin-Tsai Equations . . . . . 4

EXPERIMENTAL DETERMINATION OF ELASTIC CONSTANTS . . . . . 5

2.1 Experimental Determination of  $E_{11}$  and  $\nu_{12}$  . . . . . 6

2.2 Experimental Determination of  $E_{22}$  and  $G_{23}$  . . . . . 6

2.3 Experimental Determination of the Longitudinal  
Shear Modulus  $G_{12}$  . . . . . 7

CONCLUSIONS . . . . . 8

REFERENCES . . . . . 10

NOMENCLATURE . . . . . 12

APPENDIX I . . . . . 13

APPENDIX II . . . . . 23

APPENDIX III . . . . . 25

ACKNOWLEDGMENTS . . . . . 35

FIGURE CAPTIONS . . . . . 36



THEORETICAL AND EXPERIMENTAL DETERMINATION OF MECHANICAL  
PROPERTIES OF SUPERCONDUCTING COMPOSITE WIRE\*

W. H. Gray and C. T. Sun†

ABSTRACT

The object of this research is to characterize the mechanical properties of a composite superconducting (NbTi/Cu) wire in terms of the mechanical properties of each constituent material. For a particular composite superconducting wire, five elastic material constants were experimentally determined and theoretically calculated.

Since the Poisson's ratios for the fiber and the matrix material were very close, there was essentially no (less than 1%) difference among all the theoretical predictions for any individual mechanical constant. Because of the expense and difficulty of producing elastic constant data of 0.1% accuracy, and therefore conclusively determining which theory is best, no further experiments were performed.

INTRODUCTION

The object of this research is to characterize the mechanical properties of a composite superconducting (NbTi/Cu) wire in terms of the mechanical properties of each constituent material. In 1973, the Cryogenics Division of the National Bureau of Standards (NBS) published an interim report<sup>1</sup> in which a preliminary investigation of the mechanical properties of a solenoid coil composite was made. The coil investigated consisted of epoxy, fiberglass, and composite superconducting wire. Both theoretical and experimental elastic constants were tabulated

---

\* This research was sponsored in part by the Engineering Research Institute, Iowa State University, Ames, IA 50011, and in part by the Energy Research and Development Administration under contract with Union Carbide Corporation.

† Department of Engineering Sciences and Mechanics and Engineering Research Institute, Iowa State University, Ames, IA 50011.

for a typical piece of coil cut out of a small solenoid. Our report differs from this NBS work in that we consider only the mechanical properties of an individual composite superconducting wire.

The theoretical predictions and the experimental procedures to determine the effective elastic constants of the composite wire are described in the next two sections of this report.

## THEORETICAL INVESTIGATION

Most of the analytical work for predicting the mechanical and thermal properties of fiber-reinforced composites in terms of volumetric composition, geometrical arrangement of the fibers, and constituent material properties was done before 1970. There are five approaches to predict the micromechanical behavior of fiber-reinforced composites.\* The essential characteristic of each is described below.

### 1.1 SELF-CONSISTENT MODEL METHODS

This method was originally proposed by Hershey<sup>3</sup> and Kroner<sup>4</sup> for crystal aggregates, and was first employed by Hill<sup>5</sup> to derive expressions for elastic constants. Hill modeled the composite as a single fiber embedded in an unbounded macroscopically homogeneous medium, subjected to a uniform loading at infinity. This uniform loading produces a uniform strain field in the filament which is then used to estimate the elastic constants. A similar model proposed by Frohlich and Sack<sup>6</sup> for predicting the viscosity of a Newtonian fluid containing a dispersion of equal elastic spheres consists of three concentric cylinders, the outer one being unbounded. The innermost cylinder is assumed to have the elastic properties of the filaments; the middle one has the properties of the matrix; and the outermost has the properties of the composite. The solid is subjected to homogeneous stresses at infinity. The resulting elastic fields are determined, and then are

---

\* No attempt is made here to give a comprehensive literature survey regarding this subject. More references can be found in Ref. 2.

employed to predict the elastic constants of the composite. Applications of the self-consistent model methods can be found, for example, in Refs. 7-9.

## 1.2 VARIATIONAL METHODS

In this method, the energy theorems of classical elasticity are used to obtain bounds on the mechanical and physical properties of filamentary composites. The minimum complementary energy theorem yields a lower bound, while the minimum potential energy theorem yields the upper bound. Using this approach, bounds for the elastic and thermal properties of composites have been obtained by many investigators.<sup>10-12</sup>

## 1.3 EXACT METHODS

By assuming that the fibers are arranged in a doubly periodic rectangular array, a fundamental or repeating element can be established. The resulting elasticity problem can then be solved either by introducing a stress function using a series development, or by numerical techniques such as finite difference or finite element methods. Once the problem is solved elastically, the resulting elastic fields can be averaged to get expressions for the desired elastic constants. Typical applications of this method can be found in Refs. 13-18.

## 1.4 MECHANICS OF MATERIALS METHOD

By making simplifying assumptions regarding the mechanical or thermal behavior of a composite material, the mechanics-of-materials expressions for the equivalent elastic or thermal constants of unidirectionally reinforced fibrous composite materials can be derived. For example, to determine the longitudinal Young's modulus, one assumes that the longitudinal strains in both the matrix and the fiber are the same; in order to determine the transverse Young's modulus, one assumes that transverse stresses in both materials are the same. This approach

usually is referred to as the "rule of mixtures." The "rule of mixtures" expressions for elastic moduli and thermal conductivities can be found in Refs. 19-21.

### 1.5 THE HALPIN-TSAI EQUATIONS

For designers, it is often necessary to have simple and rapid computational procedures for estimating the macromechanical properties of a fibrous composite. Such empirical formulas have been developed by Halpin and Tsai<sup>22</sup> based upon modifications of the results discussed under approaches 1.1 and 1.3. By estimating the value of a factor which depends on the geometry of the inclusions, spacing geometry, and loading conditions, the composite elastic moduli can be approximated. Reliable estimates for this factor can be obtained by comparing the Halpin-Tsai equation with the numerical micromechanics solutions. If used appropriately, the Halpin-Tsai equation can yield very reliable results without elaborate calculations.

All the above methods make the following three basic assumptions: (1) each constituent material behaves linearly elastically, (2) the fibers are straight (without twist), and (3) there are no residual stresses. For this investigation, we use several of the available theoretical equations to predict the effective elastic mechanical properties of superconducting composite wire. These equations are listed in Appendix I.

In general, a superconducting composite wire may be twisted to minimize ac power losses in a superconducting magnet. Twisting of the wire violates an assumption implicit in the derivation of all the equations presented in Appendix I. However, we believe that this effect is small (see Appendix II), and for engineering purposes can be neglected. Other effects, such as inelastic behavior of the wire at higher loading levels, and residual stresses in the wire introduced during fabrication, may influence the results presented in this paper, and should be analyzed more thoroughly.

## EXPERIMENTAL DETERMINATION OF ELASTIC CONSTANTS

Assuming the NbTi/Cu wire behaves like a transversely isotropic material, there are five elastic constants of significance. These constants are: (1) Young's modulus along the direction of the fiber,  $E_L$  or  $E_{11}$  (longitudinal Young's modulus), (2) major Poisson's ratio,  $\nu_L$  or  $\nu_{12}$ , (3) Young's modulus along the direction normal to the fiber,  $E_T$  or  $E_{22}$  (transverse Young's modulus), (4) minor Poisson's ratio,  $\nu_T$  or  $\nu_{23}$ , and (5) longitudinal shear modulus,  $G_L$  or  $G_{12}$ . Since the material properties in a plane normal to the fiber direction are assumed to be isotropic, the transverse shear modulus  $G_T$  or  $G_{23}$  can be determined from the isotropic relation

$$G_T = \frac{E_T}{2(1 + \nu_T)} \quad (1)$$

The particular superconducting composite wire chosen for our experiment was KRYO-210.<sup>\*†23</sup> This conductor has cross-sectional dimensions of 10.16 mm by 5.08 mm with a copper matrix containing 2640 Nb-45 wt % Ti superconducting filaments. The copper to superconductor ratio is 6. The elastic constants which were used for the comparisons are tabulated below. All elastic constant measurements were made at room temperature.

Material	Young's Modulus (GPa)	Poisson's Ratio	Shear Modulus (GPa)
Cu	123	0.345	45.7
NbTi	84	0.33	31.5

---

\* Registered trademark of Magnetics Corporation of America (MCA).

† Tradenames of material are used in this report for clarity. In no case does such selection imply recommendations or endorsement by the authors, nor does it imply that the material is necessarily the best available for the purpose.

## 2.1 EXPERIMENTAL DETERMINATION OF $E_{11}$ AND $\nu_{12}$

$E_{11}$  and  $\nu_{12}$  can be determined from a simple tension test (see Fig. 1). The direction of loading is parallel to the fibers of the conductor. The longitudinal Young's modulus is determined from a  $\sigma_1$  vs  $\epsilon_1$  diagram where  $\sigma_1$  is equal to the applied load divided by the cross sectional area of the specimen, and  $\epsilon_1$  is the strain along the fiber direction of the conductor. Figure 2 represents an experimentally determined plot of this diagram for KRYO-210 superconductor showing a value for  $E_{11}$  of 119 GPa. A comparison of the theoretical prediction and the experimental data is shown in Fig. 3 in this graph, as well as the four normalized comparison graphs which follow; the legend refers to the theoretical equations presented in Appendix I. Both equations predict the same behavior, which deviates approximately 3% from the experimental data.

The major Poisson's ratio is determined from the slope of the  $\epsilon_2$  vs  $\epsilon_1$  diagram during the same experiment, where  $\epsilon_2$  is the strain in either transverse direction. The experimentally determined value was 0.347 (see Fig. 4). The normalized plot (see Fig. 5) showing the comparison between theoretical prediction and experimental value again demonstrates little difference between theories with the experimental data differing from the predictions by about 2%.

## 2.2 EXPERIMENTAL DETERMINATION OF $E_{22}$ AND $G_{23}$

$E_{22}$  and  $G_{23}$  are determined from a test similar to that described in 2.1 (see Fig. 6). The direction of the applied load is normal to the fiber axis. The transverse Young's modulus is determined from the  $\sigma_2$  vs  $\epsilon_2$  diagram where  $\sigma_2$  is the stress, and  $\epsilon_2$  is the strain in the direction of the applied force. Figure 7 represents an experimentally determined plot of this diagram for KRYO-210 superconductor showing a value for  $E_{22}$  of 122 GPa. The experimental data are compared to the theoretical predictions for  $E_{22}$  in Figure 8. An error of approximately 5% is observed.

Analogously the minor Poisson's ratio, and therefore  $G_{23}$ , is determined from an  $\epsilon_3$  vs  $\epsilon_2$  diagram. The experimental value for  $G_{23}$  is 43.1 GPa (see Fig. 9). Figure 10 compares this data point with the

theoretical predictions. An error of approximately 2% is observed.

### 2.3 EXPERIMENTAL DETERMINATION OF THE LONGITUDINAL SHEAR MODULUS $G_{12}$

The simplest way to determine the longitudinal shear modulus  $G_{12}$  is to use a tensile specimen with the fibers oriented at a  $45^\circ$  direction to the geometrical axis of the specimen.<sup>24</sup> A realistic specimen of a composite superconductor, however, would be very difficult and expensive to fabricate. An alternate method to evaluate  $G_{12}$  experimentally is outlined below.

From the two-dimensional anisotropic stress-strain relation, we have

$$\begin{Bmatrix} \epsilon_\theta \\ \epsilon_{\theta+\pi/2} \\ \gamma_\theta \end{Bmatrix} = \begin{bmatrix} \bar{s}_{11} & \bar{s}_{12} & \bar{s}_{16} \\ \bar{s}_{12} & \bar{s}_{22} & \bar{s}_{26} \\ \bar{s}_{16} & \bar{s}_{26} & \bar{s}_{66} \end{bmatrix} \begin{Bmatrix} \sigma_\theta \\ \sigma_{\theta+\pi/2} \\ \tau_\theta \end{Bmatrix} \quad (2)$$

where  $\epsilon_\theta$  and  $\epsilon_{\theta+\pi/2}$  are the axial strains of  $x'$  and  $z'$  axes. These lie in the  $xz$  plane and make angles  $\theta$  and  $\theta + \pi/2$  with the  $x$ -axis respectively;  $\gamma_\theta$  is the shear strain of  $x'$  and  $z'$  axes, and  $\sigma_\theta$ ,  $\sigma_{\theta+\pi/2}$  and  $\tau_\theta$  are the corresponding normal and shear stresses respectively (see Figure 11). The matrix  $[\bar{S}]$  in Eq. (2) represents the compliance matrix of the composite material in  $x'z'$  directions. In a simple tension test with the applied load and the fibers oriented along the  $x$  direction,  $\epsilon_\theta$  and  $\epsilon_{\theta+\pi/2}$  can be measured directly and  $\gamma_\theta$  can be computed, using the data obtained from strain gage rosette readings. For axial tension,  $\sigma_\theta$ ,  $\sigma_{\theta+\pi/2}$  and  $\tau_\theta$  are given by

$$\begin{aligned} \sigma_\theta &= \sigma_x \cos^2\theta \\ \sigma_{\theta+\pi/2} &= \sigma_x \sin^2\theta \\ \tau_\theta &= -\sigma_x \sin\theta\cos\theta \end{aligned} \quad (3)$$

where  $\sigma_x$  is equal to the applied force divided by the cross sectional area of the specimen. The elastic compliances  $\bar{S}_{11}$ ,  $\bar{S}_{12}$ ,  $\bar{S}_{22}$ ,  $\bar{S}_{16}$ ,  $\bar{S}_{26}$ , and  $\bar{S}_{66}$  are related to  $E_{11}$ ,  $E_{22}$ ,  $\nu_{12}$ , and  $G_{12}$  by the following relations.<sup>2</sup>

$$\bar{S}_{11} = \frac{\cos^4\theta}{E_{11}} + 2\left(\frac{1}{G_{12}} - \frac{\nu_{12}}{E_{11}}\right)\sin^2\theta\cos^2\theta + \frac{\sin^4\theta}{E_{22}} \quad (4)$$

$$\bar{S}_{12} = \left(\frac{1}{E_{11}} + \frac{1}{E_{22}} - \frac{2}{G_{12}}\right)\sin^2\theta\cos^2\theta - \frac{\nu_{12}}{E_{11}}(\sin^4\theta + \cos^4\theta) \quad (5)$$

$$\bar{S}_{22} = \frac{\sin^4\theta}{E_{11}} + 2\left(\frac{1}{G_{12}} - \frac{\nu_{12}}{E_{11}}\right)\sin^2\theta\cos^2\theta + \frac{\cos^4\theta}{E_{22}} \quad (6)$$

$$\bar{S}_{16} = \left(\frac{1}{E_{11}} + \frac{\nu_{12}}{E_{11}} - \frac{1}{G_{12}}\right)\sin\theta\cos^3\theta + \left(\frac{1}{G_{12}} - \frac{\nu_{12}}{E_{11}} - \frac{1}{E_{22}}\right)\sin^3\theta\cos\theta \quad (7)$$

$$\bar{S}_{26} = \left(\frac{1}{E_{11}} + \frac{\nu_{12}}{E_{11}} - \frac{1}{G_{12}}\right)\sin^3\theta\cos\theta + \left(\frac{1}{G_{12}} - \frac{\nu_{12}}{E_{11}} - \frac{1}{E_{22}}\right)\sin\theta\cos^3\theta \quad (8)$$

$$\bar{S}_{66} = \left(\frac{1}{E_{11}} + \frac{1}{E_{22}} + \frac{2\nu_{12}}{E_{11}} - \frac{1}{G_{12}}\right)\sin^2\theta\cos^2\theta + \frac{1}{2G_{12}}(\sin^4\theta + \cos^4\theta) \quad (9)$$

Since  $E_{11}$ ,  $E_{22}$ , and  $\nu_{12}$  are determined from tests (2.1) and (2.2), and  $\epsilon_\theta$ ,  $\epsilon_{\theta + \pi/2}$ ,  $\gamma_\theta$ ,  $\sigma_\theta$ ,  $\sigma_{\theta + \pi/2}$ , and  $\tau_\theta$  are obtained either from direct measurement by strain gages or from Eq. (3), the only unknown in Eq. (2) is  $G_{12}$ . Thus  $G_{12}$  can be computed from any one of the three equations in Eq. (2). Its value is found to be 44.8 GPa which is within 5% of the theoretical predictions (see Fig. 12).

### CONCLUSIONS

The goal of this experiment was to determine which theory of composites best predicted the elastic mechanical behavior of a superconducting (NbTi/Cu) composite wire. Examination of each elastic mechanical property reveals that all theories examined are capable of predicting experimental data to within 5%.

Since the Poisson's ratios for both the fiber and the matrix material were very close, there was essentially no (less than 1%) difference among all the theoretical predictions for any individual mechanical constant. Because of the expense and difficulty of producing elastic constant data within 0.1% accuracy, and therefore, conclusively determining which theory is best, no further experiments were performed.

In conclusion, for a superconducting composite wire, NbTi/Cu, a simple, fast, and reliable engineering estimate of its elastic mechanical behavior can be made by using the "rule of mixtures." It is unnecessary to use one of the more rigorous theories.

#### REFERENCES

1. C. W. Fowlkes et al., "Characterization of a Superconducting Coil Composite," NBSIR-73-349, Boulder, Colorado (1973).
2. J. E. Ashton, J. C. Halpin, and P. H. Petit, Primer on Composite Materials: Analysis, Technomic Publishing Co., Stamford, Connecticut (1969).
3. A. V. Hershey, "The Elasticity of an Isotropic Aggregate of Anisotropic Cubic Crystals," J. of Appl. Mech. 21, 235 (1954).
4. E. Kroner, "Berechnung der Elastischen Konstanten des Vielkristalls aus den Konstanten des Einkristalls," Z. Phys. 151, 504 (1958).
5. R. Hill, "Theory of Mechanical Properties of Fiber-strengthened Materials Self-consistent Model," Journal of Mechanics and Physics of Solids 13, 189 (1965).
6. H. Frohlich and B. Sack, "Theory of the Rheological Properties of Dispersion," Proc. R. Soc. Lond. A185, 415 (1946).
7. J. J. Hermann, "The Elastic Properties of Fiber Reinforced Materials When the Fibers are Aligned," Proceedings Koninklijke Nederlands Akademische van Wetenschappen, Amsterdam Series B. 70(1), 1 (1967).
8. Z. Hashin, "Assessment of the Self-consistent Scheme Approximation - Conductivity of Particulate Composites," Journal of Composite Materials 2, 284 (1968).
9. Z. Hashin and W. Rosen, "The Elastic Moduli of Fiber-Reinforced Materials," J. of Appl. Mech. 31, 223 (1964).
10. Z. Hashin, "On Elastic Behavior of Fiber-Reinforced Materials of Arbitrary Transverse Phase Geometry," Journal of Mechanics and Physics of Solids 13, 119 (1965).
11. R. A. Schapery, "Thermal Expansion Coefficients of Composite Materials Based on Energy Principle," Journal of Composite Materials 2(3), 380 (1968).
12. R. Hill, "Theory of Mechanical Properties of Fiber-Strengthened Materials: Elastic Behavior," Journal of Mechanical Physics of Solids 2, 199 (1964).
13. D. F. Adams and D. R. Doner, "Longitudinal Shear Loading of a Unidirectional Composite," Journal of Composite Materials 1, 152 (1967).

14. D. F. Adams and D. R. Doner, "Transverse Normal Loading of a Unidirectional Composite," *Journal of Composite Materials* 1, 152 (1967).
15. C. H. Chen and S. Cheng, "Mechanical Properties of Fiber-Reinforced Composites," *Journal of Composite Materials* 1, 30 (1967).
16. E. Behrens, "Thermal Conductivity of Composite Materials," *Journal of Composite Materials* 2(1), 2 (1968).
17. S. I. Kang and G. M. Rentzepis, "On the Determination of Physical Properties of Composite Materials by a Three-Dimensional Finite Element Procedure," *Composite Materials: Testing and Design*, American Society for Testing and Materials Special Technical Publication S46, Philadelphia, Pennsylvania (1973).
18. R. M. Barker, F. T. Lin and J. R. Dana, "Three-Dimensional Finite-Element Analysis of Laminated Composites," *Computers and Structures* 2, 1013-1029 (1972).
19. R. M. Jones, Mechanics of Composite Materials, McGraw-Hill, New York (1974).
20. J. C. Ekvall, "Elastic Properties of Orthotropic Monofilament Laminates," paper 61-AV56 presented at American Society of Mechanical Engineers Aviation Conference, Los Angeles, California (March 1961).
21. G. S. Springer and S. W. Tsai, "Thermal Conductivity of Unidirectional Materials," *Journal of Composite Materials* 1, 166 (1967).
22. J. C. Halpin and S. W. Tsai, "Environmental Factors in Composite Materials Design," AFML-TR-67-423, Air Force Materials Laboratory, (1967).
23. G. A. Miranda and J. D. Rogers, "Adjacent Conductor Field Corrections to High Critical Current Short Sample Measurements," LA-UR-74-1413, Los Alamos, New Mexico (1974).
24. B. W. Rosen, "A Simple Procedure for Experimental Determination of the Longitudinal Shear Modulus of Unidirectional Composites," *Journal of Composite Materials* 6, 552 (October 1972).
25. J. M. Whitney, "Geometrical Effects of Filament Twist on the Modulus and Strength of Graphite Fiber-Reinforced Composites," *Textile Research Journal* 36(9), 765 (September 1966).

## NOMENCLATURE

### Symbol Definition

- E - Young's modulus
- G - Shear modulus
- $\nu$  - Poisson's ratio
- K - Bulk modulus in plane strain
- V - Volume fraction
- f - Fiber material (NbTi)
- m - Matrix material (Cu)
- L - Composite material constants along the fiber direction
- T - Composite material constants along a transverse direction

## APPENDIX I

This appendix presents the various theoretical equations which were used to predict the elastic mechanical properties for the superconducting composite wire studied in this report. Their alphabetic index refers to the legend on the particular graph where a comparison with experimental data was performed. Also included in this appendix is the reference in which these equations may be found.

A program which numerically tabulates all of these equations is listed in Appendix III.

1. Longitudinal Young's modulus  $E_L$

$$(a) \quad E_L = E_m V_m + E_f V_f \quad (10)$$

Source: Reference 2

$$(b) \quad E_L = \left( E_m V_m + E_f V_f \right) \phi \quad (11)$$

$$\phi = \frac{E_m (D_1 - D_3 F_1) + E_f (D_2 - D_4 F_2)}{E_m (D_1 - D_3) + E_f (D_2 - D_4)}$$

$$D_1 = 1 - \nu_f \quad D_2 = \frac{1 + \nu_f}{\nu_m} + \nu_m$$

$$D_3 = 2\nu_f^2 \quad D_4 = 2\nu_m^2 \frac{\nu_f}{\nu_m}$$

$$F_1 = \frac{\nu_m \nu_f E_f + \nu_f \nu_m E_m}{\nu_f E_f \nu_f + \nu_m E_m \nu_f}$$

$$F_2 = \frac{\nu_f}{\nu_m} F_1$$

Source: Reference 10

2. Major Poisson's ratio  $\nu_L$

$$(a) \quad \nu_L = \frac{V_f E_f L_1 + V_m E_m \nu_m L_2}{V_f E_f L_3 + V_m E_m L_2} \quad (12)$$

$$L_1 = 2\nu_f(1 - \nu_m^2)V_f + \nu_m(1 + \nu_m)V_m$$

$$L_2 = (1 - \nu_f - 2\nu_f^2)V_f$$

$$L_3 = 2(1 - \nu_m^2)V_f + (1 + \nu_m)V_m$$

Source: Reference 10

$$(b) \quad \nu_L = \nu_m V_m + \nu_f V_f \quad (13)$$

Source: Reference 2

### 3. Transverse Young's modulus $E_T$

$$(a) \quad E_T = \frac{E_f E_m}{E_f V_m + E_m V_f} \quad (14)$$

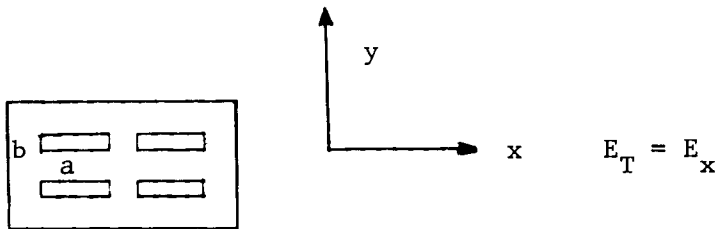
Source: Reference 23

$$(b) \quad E_T = \frac{1 + \phi \eta V_f}{1 - \eta V_f} E_m \quad (15)$$

$$\eta = \frac{\frac{E_f}{E_m} - 1}{\frac{E_f}{E_m} + \phi}$$

$\phi = 2$  for circular fiber

$\phi = 2\left(\frac{a}{b}\right)$  for rectangular fiber



Source: Reference 2

$$(c) \quad E_T = 2 \left[ 1 - \nu_f + (\nu_f - \nu_m) V_m \right] \frac{M_f (2M_m + G_m) - G_m (M_f - M_m) V_m}{2M_m + G_m + 2(M_f - M_m) V_m} \quad (16)$$

$$M_f = \frac{E_f}{2(1 - \nu_f)} \quad M_m = \frac{E_m}{2(1 - \nu_m)}$$

Source: Reference 23

$$(d) \quad \frac{E_T}{E_m} = \left(1 - 2\sqrt{\frac{V_f}{\pi}}\right) + \frac{1}{\alpha} \left\{ \pi - \frac{4}{\sqrt{1 - \frac{\alpha^2 V_f}{\pi}}} \tan^{-1} \left[ \frac{\sqrt{1 - (\alpha^2 V_f / \pi)}}{1 + \sqrt{\alpha^2 V_f / \pi}} \right] \right\} \quad (17)$$

$$\alpha = 2 \left( \frac{E_m}{E_f} - 1 \right)$$

Source: Reference 23

$$(e) \quad \frac{1}{E_T} = \frac{V_m}{E_m} + \frac{V_f}{E_f} - \frac{V_f}{E_f} \frac{\left( \frac{E_f}{E_m} v_m - v_f \right)^2}{\frac{V_f E_f}{V_m E_m} + 1} \quad (18)$$

Source: Reference 23

4. Transverse shear modulus  $G_T$

$$(a) \quad G_T \text{ (lower bound)} = G_m \left[ 1 - \frac{2(1 - \nu_m)}{1 - 2\nu_m} \nu_f A_4^\varepsilon \right] \quad (19)$$

where  $A_4^\varepsilon$  is obtained by solving the following equations

$$[P] \begin{Bmatrix} A_1 \\ A_2 \\ A_3 \\ \varepsilon \\ A_4 \\ B_1 \\ B_2 \end{Bmatrix} = \begin{Bmatrix} 1 \\ 0 \\ 0 \\ 0 \\ 0 \\ 0 \\ 0 \end{Bmatrix}$$

$$\text{where } [P] = \begin{bmatrix} 1 & \nu_f^{-1} & \nu_f^2 & \nu_f & 0 & 0 \\ 0 & \frac{1}{\nu_f} \frac{4\nu_m - 3}{3 - 2\nu_m} & -2\nu_f^2 & \frac{\nu_f}{1 - 2\nu_m} & 0 & 0 \\ 1 & 1 & 1 & 1 & -1 & -1 \\ 0 & \frac{4\nu_m - 3}{3 - 2\nu_m} & -2 & \frac{1}{1 - 2\nu_m} & 0 & \frac{3 - 4\nu_f}{3 - 2\nu_f} \\ 1 & \frac{3}{3 - 2\nu_m} & -3 & \frac{1}{1 - 2\nu_m} & -\frac{G_f}{G} & \frac{3 G_f / G_m}{2\nu_f - 3} \\ 0 & -\frac{1}{3 - 2\nu_m} & 2 & \frac{-1}{1 - 2\nu_m} & 0 & \frac{G_f / G_m}{3 - 2\nu_f} \end{bmatrix}$$

Source: Reference 10

$$(b) \quad G_T \text{ (upper bound)} = G_m \left[ \frac{1}{1 + \frac{2(1 - \nu_m)}{1 - 2\nu_m} V_f A_4^\sigma} \right] \quad (20)$$

and  $A_4^\sigma$  is obtained by solving

$$[R] \begin{Bmatrix} A_1 \\ A_2 \\ A_3 \\ A_4^\sigma \\ B_1 \\ B_2 \end{Bmatrix} = \begin{Bmatrix} 1 \\ 0 \\ 0 \\ 0 \\ 0 \\ 0 \end{Bmatrix}$$

where

$$[R] = \begin{bmatrix} 1 & \frac{3}{3 - 2\nu_m} \frac{1}{V_f} & -3V_f^2 & \frac{V_f}{1 - 2\nu_m} & 0 & 0 \\ 0 & \frac{-1}{3 - 2\nu_m} \frac{1}{V_f} & 2V_f^2 & \frac{-V_f}{1 - 2\nu_m} & 0 & 0 \\ 1 & 1 & 1 & 1 & -1 & -1 \\ 0 & \frac{4\nu_m - 3}{3 - 2\nu_m} & -2 & \frac{1}{1 - 2\nu_m} & 0 & \frac{3 - 4\nu_f}{3 - 2\nu_f} \\ 1 & \frac{3}{3 - 2\nu_m} & -3 & \frac{1}{1 - 2\nu_m} & -\frac{G_f}{G_m} & \frac{3 G_f / G_m}{2\nu_f - 3} \\ 0 & -\frac{1}{3 - 2\nu_m} & 2 & \frac{-1}{1 - 2\nu_m} & 0 & \frac{G_f / G_m}{3 - 2\nu_f} \end{bmatrix}$$

Source: Reference 10

$$(c) \quad G_T = G_m \frac{2G_f(K_m + G_m)V_f + 2G_m G_f V_m + K_m V_m (G_m + G_f)}{2G_m(K_m + G_m)V_f + 2G_m G_f V_m + K_m V_m (G_m + G_f)} \quad (21)$$

Source: Reference 7

$$(d) \quad G_T \text{ (lower bound)} = G_m + \frac{V_f}{\frac{1}{G_f - G_m} + \frac{(K_m + 2G_m V_m)}{2G_m(K_m + G_m)}} \quad (22)$$

Source: Reference 11

$$(e) \quad G_T \text{ (upper bound)} = G_f + \frac{V_m}{\frac{1}{G_m - G_f} + \frac{K_f + 2G_f V_f}{2G_f(K_f + G_f)}} \quad (23)$$

Source: Reference 11

5. Longitudinal shear modulus  $G_L$

$$(a) \quad G_L = \frac{G_f (1 + V_f) + V_m}{\frac{G_f}{G_m} V_m + 1 + V_f} \quad (24)$$

Source: Reference 10

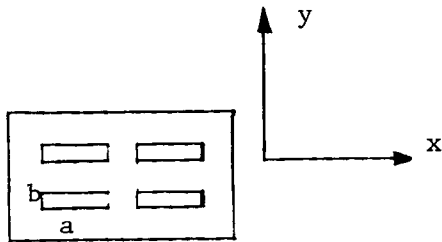
$$(b) \quad G_L = \frac{G_f G_m}{V_m G_f + V_f G_m} \quad (25)$$

Source: Reference 23

$$(c) \quad G_L = \frac{1 + \phi \eta V_f}{1 - \eta V_f} G_m \quad (26)$$

$$\eta = \left( \frac{G_f}{G_m} - 1 \right) / \left( \frac{G_f}{G_m} + \phi \right)$$

$$\phi = \left( \frac{a}{b} \right)^{\sqrt{3}} \text{ for rectangular fiber}$$



$$G_L = G_{XZ}$$

$$\phi = 1 \text{ for circular fiber}$$

Source: Reference 2

$$(d) \quad G_L = \frac{2G_f - (G_f - G_m) \frac{V_m}{V_m} G_m}{2G_m + (G_f - G_m) \frac{V_m}{V_m} G_m} \quad (27)$$

Source: Reference 10

$$(e) \quad G_L \text{ (lower bound)} = G_m + \frac{\frac{V_f}{G_f - G_m} + \frac{V_m}{2G_m}}{\frac{1}{G_f - G_m} + \frac{V_m}{2G_m}} \quad (28)$$

Source: Reference 11

$$(f) \quad G_L \text{ (upper bound)} = G_f + \frac{\frac{V_m}{G_m - G_f} + \frac{V_f}{2G_f}}{\frac{1}{G_m - G_f} + \frac{V_f}{2G_f}} \quad (29)$$

Source: Reference 11

$$(g) \quad G_L = \frac{G_m}{2} \left[ \frac{4 - \pi + \pi\phi}{4} + \frac{\phi}{\phi(4 - \pi) + \pi} \right] \quad (30)$$

$$\phi = \frac{G_f (\pi + 4V_f) + (G_m \pi - 4V_f)}{G_f (\pi - 4V_f) + (G_m \pi + 4V_f)}$$

Source: Reference 23

## APPENDIX II

Whitney<sup>25</sup> has investigated the influence of twist on graphite fibers in an epoxy matrix. He derived an equation for the reduction of the longitudinal elastic Young's modulus for graphite as a function of the geometry of the fibers. This equation is directly applicable in estimating how twisting affects a superconducting wire.

If the initial and reduced moduli are  $E_I$  and  $E_R$ , respectively, then their ratio can be expressed as:<sup>25</sup>

$$\frac{E_R}{E_I} = \frac{1}{1 + 4\pi^2 N_o^2 R^2},$$

where  $N_o$  is the number of twists per centimeter and  $R$  is the radius of the fiber in centimeters.

For the superconducting wire analyzed in this report,

$$N_o = .132 \text{ cm}^{-1}$$

$$R = 3.17 \times 10^{-3} \text{ cm},$$

which yields

$$\frac{1}{1 + 4\pi^2 N_o^2 R^2} = \frac{1}{1 + 6.87 \times 10^{-6}} \approx 1.$$

Clearly, the effect of twist for this superconducting wire can be neglected.



APPENDIX III



```

C
C PROGRAM FIBERC.V1A
C
C LAST UPDATED: 1APR76
C
C AUTHOR: W. H. GRAY
C         P. O. BOX Y 9204-1
C         OAK RIDGE NATIONAL LABORATORY
C         OAK RIDGE, TN. 37830
C
C LANGUAGE: DECSYSTEM-10, FORTRAN-10
C
C SUBROUTINES REQUIRED:
C
C     MINV - STANDARD IBM SCIENTIFIC SUBROUTINE PACKAGE.
C
C     IMPLICIT REAL (K)
C     REAL NUF,NUM
C     DIMENSION U(6,6),RES(6),L(6),M(6),A(6)
C     DIMENSION UINV(6,6)
C     DIMENSION ELEM(2),XNULT(2),GLGM(7),GTGM(5),
1  KTKM(4),ELEM(5)
C     DATA PI/3.1415926/
C     DATA IORED,IOURT/5,5/
C
C BEGIN PROGRAM FIBERC.V1A
C
C QUERY THE USER FOR THE MATERIAL PROPERTIES
C     WRITE(IOURT, 11)
11  FORMAT(// 'FIBERC.V1A DOCUMENTED IN ORNL/TM-5331'//
1  ' INPUT IN THE FOLLOWING ORDER:'//
2  ' EF(FIBER YOUNGS MODULUS)'//
3  ' EM(MATRIX YOUNGS MODULUS)'//
4  ' NUF(FIBER POISSONS RATIO)'//
5  ' NUM(MATRIX POISSON RATIO)'//
6  ' VF(FIBER VOLUME FRACTION)'//
7  ' ORDER IS EF,EM,NUF,NUM,VF FORMAT(SF)'//
8  ' REMEMBER A SPACE DELIMITS THE INPUT VARIABLES'//)
10  READ(IORED,10)EF,EM,NUF,NUM,VF
989  FORMAT(SF)
C     CONTINUE
C
C CALCULATE THE SHEAR MODULII
C     GF=EF/(2.*(1.+NUF))
C     GM=EM/(2.*(1.+NUM))
C
C CALCULATE THE MATRIX VOLUME FRACTION
C     VM=1.-VF
C
C CALCULATE THE BULK MODULII
C     KF=EF/(3.*(1.-2.*NUF))
C     KM=EM/(3.*(1.-2.*NUM))
C
C CALCULATE THE FIBER-MATRIX RATIOS.
C     GMGF=GM/GF
C     GFGM=GF/GM
C     EFEM=EF/EM
C     EMEF=EM/EF
C     GMEM=GM/EM
C     KMGM=KM/GM
C     KFGF=KF/GF

```

```

      KFGM=KF/GM
C ECHO INPUT DATA
      WRITE(10WRT,29) EF,EM,NUF,NUM,VF,GF,GM,EFEM,KF,KM,GFGM
29   FORMAT(/// INPUT DATA'//,
1*   EF = ',T10,1PE11.4,/,
2*   EM = ',T10,1PE11.4,/,
3*   NUF = ',T10,1PE11.4,/,
4*   NUM = ',T10,1PE11.4,/,
5*   VF = ',T10,1PE11.4,/,
6*   GF = ',T10,1PE11.4,/,
7*   GM = ',T10,1PE11.4,/,
8*   EF/EM = ',T10,1PE11.4,/,
9*   KF = ',T10,1PE11.4,/,
*   KM = ',T10,1PE11.4,/, GF/GM = ',T10,1PE11.4)

C
C THE EQUATION NUMBERS GIVEN IN THE REST OF THIS CODE REFER
C TO ORNL/TM-5331
C
C CALCULATE THE LONGITUDINAL YOUNG'S MODULUS
C EQUATION 10
      ELEM(1)=VF*EFEM+VM
C EQUATION 11
      IF(VM.NE.0.0) GO TO 21
      ALPHA=1.
      GO TO 20
21   CONTINUE
      F1=(NUM*VF*EFEM+NUF*VM)/(NUF*VF*EFEM+NUF*VM)
      F2=NUF*F1/NUM
      D1=1.-NUF
      D2=(1.+VF)/VM+NUM
      D3=2.*NUF*NUF
      D4=2.*NUM*NUM*VF/VM
      ALPHA=D1-D3*F1+EFEM*(D2-D4*F2)
      ALPHA=ALPHA/(D1-D3+EFEM*(D2-D4))
20   ELEM(2)=ELEM(1)*ALPHA
      WRITE(10WRT,25)
25   FORMAT(/// LONGITUDINAL MODULUS'/)
C OUTPUT DATA ON DATA FILE
      DO 801 J=1,2
801  ELEM(J)=ELEM(J)*EM
      DO 30 J=1,2
      JJ=J+9
      WRITE(10WRT,24) JJ,ELEM(J)
30   CONTINUE
24   FORMAT(1X,'EQU. ',I2,4X,1PE11.4)
C
C CALCULATE THE MAJOR POISSON RATIO
C EQUATION 12
      XL1=2.*NUF*(1.-NUM*NUM)*VF+NUM*(1.+NUM)*VM
      XL2=VF*(1.-NUF-2.*NUF*NUF)
      XL3=2.*(1.-NUM*NUM)*VF+(1.+NUM)*VM
      XNULTA=VF*EFEM*XL1+VM*NUM*XL2
      XNULT(1)=XNULTA/(VF*EFEM*XL3+VM*XL2)
C
C EQUATION 13
      XNULT(2)=VF*NUF+VM*NUM
      WRITE(10WRT,225)
225  FORMAT(/// MAJOR POISSONS RATIO'/)

```

```

C OUTPUT DATA ON DATA FILE
  DO 31 J=1,2
  JJ=J+11
  WRITE(IOWRT,24) JJ,XMULT(J)
31 CONTINUE
C
C CALCULATE THE TRANSVERSE YOUNG'S MODULUS
C
C EQUATION 14
  ETEM(1)=1./(VM+EMEF*VF)
C
C EQUATION 15
  ETA=(EFEM-1.)/(EFEM+2.)
  ETEM(2)=(1.+2.*ETA*VF)/(1.-ETA*VF)
C
C EQUATION 16
  XMF=EFEM/(2.*(1.-NUF))
  XMM=1./(2.*(1.-NUM))
  PART=2.*(1.-NUF+(NUF-NUM)*VM)
  PART=PART*(XMF*(2.*XMM+GMEM)-GMEM*(XMF-XMM)*VM)
  ETEM(3)=PART/(2.*XMM+GMEM+2.*(XMF-XMM)*VM)
C
C EQUATION 17
  ALPHA=2.*(EMEF-1.)
C
C CHECK FOR A POSITIVE RADICAL FOR SQRT.
  IF(1.-ALPHA*ALPHA*VF/PI.LE.0.) GO TO 160
  XNMR=SQRT(1.-ALPHA*ALPHA*VF/PI)
  TANSTF=ATAN2(XNMR,(1.+SQRT(ALPHA*ALPHA*VF/PI)))
  SQ=4./SQRT(1.-ALPHA*ALPHA*VF/PI)
  ETEM(4)=1.-2.*SQRT(VF/PI)+(PI-SQ*TANSTF)/ALPHA
  GO TO 161
160 CONTINUE
  ETEM(4)=-1.
161 CONTINUE
C
C EQUATION 18
  SQ=(EFEM*NUM-NUF)**2*VF/EF
  ETEM(5)=VM/EM+VF/EF-SQ/(VF*EF/VM/EM+1.)
  ETEM(5)=1./(ETEM(5)*EM)
  WRITE(IOWRT,625)
625 FORMAT(//,' TRANSVERSE YOUNGS MODULUS'//)
C OUTPUT DATA ON DATA FILE
  EHG=AMAX1(EF,EM)
  ELW=AMINI(EF,EM)
  DO 805 J=1,5
805 ETEM(J)=ETEM(J)*EM
  DO 32 J=1,5
  JJ=J+13
  IF(ETEM(J).GT.EHG.OR.ETEM(J).LT.ELW) GO TO 82
  WRITE(IOWRT,24) JJ,ETEM(J)
  GO TO 32
82 WRITE(IOWRT,83) JJ
83 FORMAT(' EQU. ',12,' NOT APPLICABLE')
32 CONTINUE
C
C CALCULATE THE TRANSVERSE SHEAR MODULUS
C
C EQUATION 19
C

```

```

C BEGIN TO SET UP THE COEFFICIENT MATRIX
  U(1,1)=1.
  U(2,1)=0.
  U(3,1)=1.
  U(4,1)=0.
  U(5,1)=1.
  U(6,1)=0.
  U(3,2)=1.
  U(3,3)=1.
  U(4,3)=-2.
  U(5,3)=-3.
  U(6,3)=2.
  U(3,4)=1.
  U(1,5)=0.
  U(2,5)=0.
  U(3,5)=-1.
  U(4,5)=0.
  U(6,5)=0.
  U(1,6)=0.
  U(2,6)=0.
  U(3,6)=-1.
  U(1,2)=1./VF
  U(4,2)=- (3.-4.*NUM)/(3.-2.*NUM)
  U(2,2)=U(4,2)/VF
  U(6,2)=-1./ (3.-2.*NUM)
  U(5,2)=-3.*U(6,2)
  U(1,3)=VF*VF
  U(2,3)=-2.*U(1,3)
  U(1,4)=VF
  U(4,4)=1./ (1.-2.*NUM)
  U(2,4)=VF*U(4,4)
  U(5,4)=U(4,4)
  U(6,4)=-U(4,4)
  U(5,5)=-GFGM
  U(4,6)= (3.-4.*NUF)/(3.-2.*NUF)
  U(6,6)=GFGM/(3.-2.*NUF)
  U(5,6)=-3.*U(6,6)
C
C STORE THE COEFFICIENT MATRIX INTO UINV
  DO 71 IH=1,6
    DO 71 JH=1,6
      UINV(IH,JH)=U(IH,JH)
71
C
C FORMULATE RIGHT HAND SIDE
  A(1)=1.
  A(2)=0.
  A(3)=0.
  A(4)=0.
  A(5)=0.
  A(6)=0.
C
C INVERT THE COEFFICIENT MATRIX. SUBROUTINE MINV IS THE STANDARD
C IBM SCIENTIFIC SUBROUTINE MATRIX INVERTER.
  CALL MINV(UINV,6,D,L,M)
C
C OBTAIN THE SOLUTION VECTOR
  DO 69 MK=1,6
    RES(MK)=0.
    DO 69 ML=1,6
      RES(MK)=A(ML)*UINV(MK,ML)+RES(MK)
69

```

```

      GTGM(1)=1.-2.*(1.-NUM)*VF*RES(4)/(1.-2.*NUM)
C
C EQUATION 20
C
C BEGIN TO SET UP THE COEFFICIENT MATRIX
      U(1,1)=1.
      U(2,1)=0.
      U(3,1)=1.
      U(4,1)=0.
      U(5,1)=1.
      U(6,1)=0.
      U(1,2)=1.
      U(1,3)=1.
      U(2,3)=-2.
      U(3,3)=-3.
      U(4,3)=2.
      U(1,4)=1.
      U(1,5)=-1.
      U(2,5)=0.
      U(4,5)=0.
      U(5,5)=0.
      U(6,5)=0.
      U(1,6)=-1.
      U(5,6)=0.
      U(6,6)=0.
      U(4,2)=-1./ (3.-2.*NUM)
      U(3,2)=-3.*U(4,2)
      U(2,2)=(3.-4.*NUM)*U(4,2)
      U(5,2)=U(3,2)/VF
      U(6,2)=U(4,2)/VF
      U(5,3)=-3.*VF*VF
      U(6,3)=2.*VF*VF
      U(2,4)=1./ (1.-2.*NUM)
      U(3,4)=U(2,4)
      U(4,4)=-U(2,4)
      U(5,4)=VF*U(2,4)
      U(6,4)=-U(5,4)
      U(3,5)=-GFGM
      U(2,6)=(3.-4.*NUF)/ (3.-2.*NUF)
      U(4,6)=GFGM/ (3.-2.*NUF)
      U(3,6)=-3.*U(4,6)
C
C STORE THE COEFFICIENT MATRIX INTO UINV.
      DO 81 IH=1,6
      DO 81 JH=1,6
B1    UINV(IH,JH)=U(IH,JH)
C
C FORMULATE THE RIGHT HAND SIDE.
      A(1)=0.
      A(2)=0.
      A(3)=0.
      A(4)=0.
      A(5)=1.
      A(6)=0.
C
C INVERT THE MATRIX.
      CALL MINV(UINV,6,D,L,M)
C
C OBTAIN THE SOLUTION VECTOR.
      DO 89 MK=1,6

```

```

RES(MK)=0.
DO 89 ML=1,6
89 RES(MK)=A(ML)*UINV(MK,ML)+RES(MK)
GTGM(2)=1./(1.+2.*(1.-NUM)/(1.-2.*NUM))*VF*RES(4)
C
C EQUATION 21
KMG1=(KMG+1.)*VF*2.
GFG1=(GFG+1.)*VM*KMG
GTGM(3)=GFG*KMG1+2.*GFG*VM+GFG1
GTGM(3)=GTGM/(KMG1+2.*GFG*VM+GFG1)
C
C EQUATION 22
GTGM(4)=1.+VF/(1./(GFG-1.)+(KMG+2.)*VM/(2.*(KMG+1.)))
C
C EQUATION 23
FRAC=((KFGF+2.)*VF/2./(KFGM+GFG)+1./(1.-GFG))
100 GTGM(5)=GFG+VM/FRAC
WRITE(IOWRT,425)
425 FORMAT(//,' TRANSVERSE SHEAR MODULUS'/)
C OUTPUT DATA ON DATA FILE
DO 803 J=1,5
803 GTGM(J)=GTGM(J)*GM
DO 33 J=1,5
JJ=J+18
WRITE(IOWRT,24) JJ,GTGM(J)
33 CONTINUE
C
C CALCULATE THE MINOR POISSON RATIO USING THE RULE OF MIXTURES
C TRANSVERSE YOUNG'S MODULUS AND EACH OF THE PREVIOUSLY CALCULATED
C TRANSVERSE SHEAR MODULI.
C
E22=EEM(1)
WRITE(IOWRT,79)
DO 75 J=1,5
JJ=J+18
C
C EQUATION 1
POI23=(E22/(2.*GTGM(J)))-1.
IF(POI23.LT.0.0.OR.POI23.GT.0.5) GO TO 76
WRITE(IOWRT,77) JJ,POI23
GO TO 75
76 WRITE(IOWRT,78) JJ
75 CONTINUE
77 FORMAT(' EQU. 1 USING EQU. ',I2,4X,1PE11.4)
78 FORMAT(' EQU. 1 USING EQU. ',I2,' NOT APPLICABLE')
79 FORMAT(//,' MINOR POISSONS RATIO'/)
C
C CALCULATE THE LONGITUDINAL SHEAR MODULUS
C
C EQUATION 24
GLGM(1)=(GFG*(1.+VF)+VM)/(GFG*VM+1.+VF)
C
C EQUATION 25
GLGM(2)=1./(VM+GMGF*VF)
C
C EQUATION 26
ETA=VF*(GFG-1.)/(GFG+1.)
GLGM(3)=(1.+ETA)/(1.-ETA)
C
C EQUATION 27

```

```

      GLGMD=2.*GFGM-(GFGM-1.)*VM
      GLGM(4)=GLGMD/(2.+(GFGM-1.)*VM)
C
C EQUATION 28
      FRAC=1./(GFGM-1.)
      GLGM(5)=1.+VF/(FRAC+VM/2.)
C
C EQUATION 29
      FRAC=1./(1.-GFGM)+VF/(2.*GFGM)
      GLGM(6)=GFGM+VM/FRAC
C
C EQUATION 30
      ALPHA=GFGM*(4.*VF+PI)+PI-4.*VF
      ALPHA=ALPHA/(GFGM*(PI-4.*VF)+PI+4.*VF)
      GLGM(7)=.5*((4.-PI+PI*ALPHA)/4.+4.*ALPHA/(ALPHA*(4.-PI)+PI))
      WRITE(IOWRT, 325)
325  FORMAT(//,' LONGITUDINAL SHEAR MODULUS'/)
C OUTPUT DATA ON DATA FILE
      GHG=AMAX1(GF,GM)
      GLW=AMIN1(GF,GM)
      DO 802 J=1,7
002  GLGM(J)=GLGM(J)*GM
      DO 34 J=1,7
      JJ=J+23
      IF(GLGM(J).GT.GHG.OR.GLGM(J).LT.GLW) GO TO 85
      WRITE(IOWRT,24) JJ,GLGM(J)
      GO TO 34
85  WRITE(IOWRT,83) JJ
34  CONTINUE
C
C MORE DATA
      WRITE(IOWRT, 990)
990  FORMAT(//' MORE DATA?'/
      1  ' INPUT EF,EM,NUF,NUM,VF FORMAT(5F)'/
      2  ' NEGATIVE EF STOPS THE PROGRAM')
      READ(IORED,10)EF,EM,NUF,NUM,VF
      IF(EF.GT.0.) GO TO 989
      STOP
      END

```



#### ACKNOWLEDGMENTS

The authors wish to thank S. E. Bolt for his assistance with the experimental aspect of this paper and C. J. Long and W.C.T. Stoddart for their useful comments during the preparation of this manuscript. We also wish to thank K. E. Rothe for her assistance with the computer program listed in Appendix III.

#### FIGURE CAPTIONS

- Fig. 1. Direction of loading for the determination of the longitudinal Young's modulus and the major Poisson's ratio.
- Fig. 2.  $\sigma_1$  vs  $\epsilon_1$  diagram for Kryo-210 superconductor.
- Fig. 3. Normalized plot of the longitudinal Young's Modulus versus volume fraction of the fiber (NbTi): In this graph, as well as the other normalized comparison graphs, the legend refers to the theoretical equations presented in Appendix I.
- Fig. 4.  $\epsilon_2$  vs  $\epsilon_1$  diagram for Kryo-210 superconductor.
- Fig. 5. Normalized plot of the major Poisson's ratio vs volume fraction of the fiber (NbTi).
- Fig. 6. Direction of loading for the determination of the transverse Young's Modulus and the minor Poisson's ratio.
- Fig. 7.  $\sigma_2$  vs  $\epsilon_2$  diagram for Kryo-210 superconductor.
- Fig. 8. Normalized plot of the transverse Young's Modulus versus volume fraction of the fiber (NbTi).
- Fig. 9.  $\epsilon_3$  vs  $\epsilon_2$  diagram for Kryo-210 superconductor.
- Fig. 10. Normalized plot of  $G_{23}$  vs the volume fraction of the fiber (NbTi).
- Fig. 11. Coordinate system for the determination of the longitudinal shear modulus.
- Fig. 12. Normalized plot of the longitudinal shear modulus vs volume fraction of the fiber (NbTi).

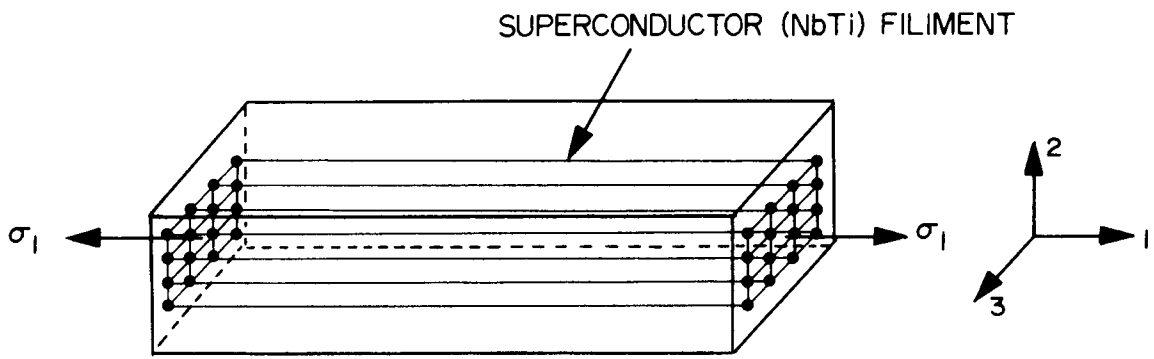


Figure 1

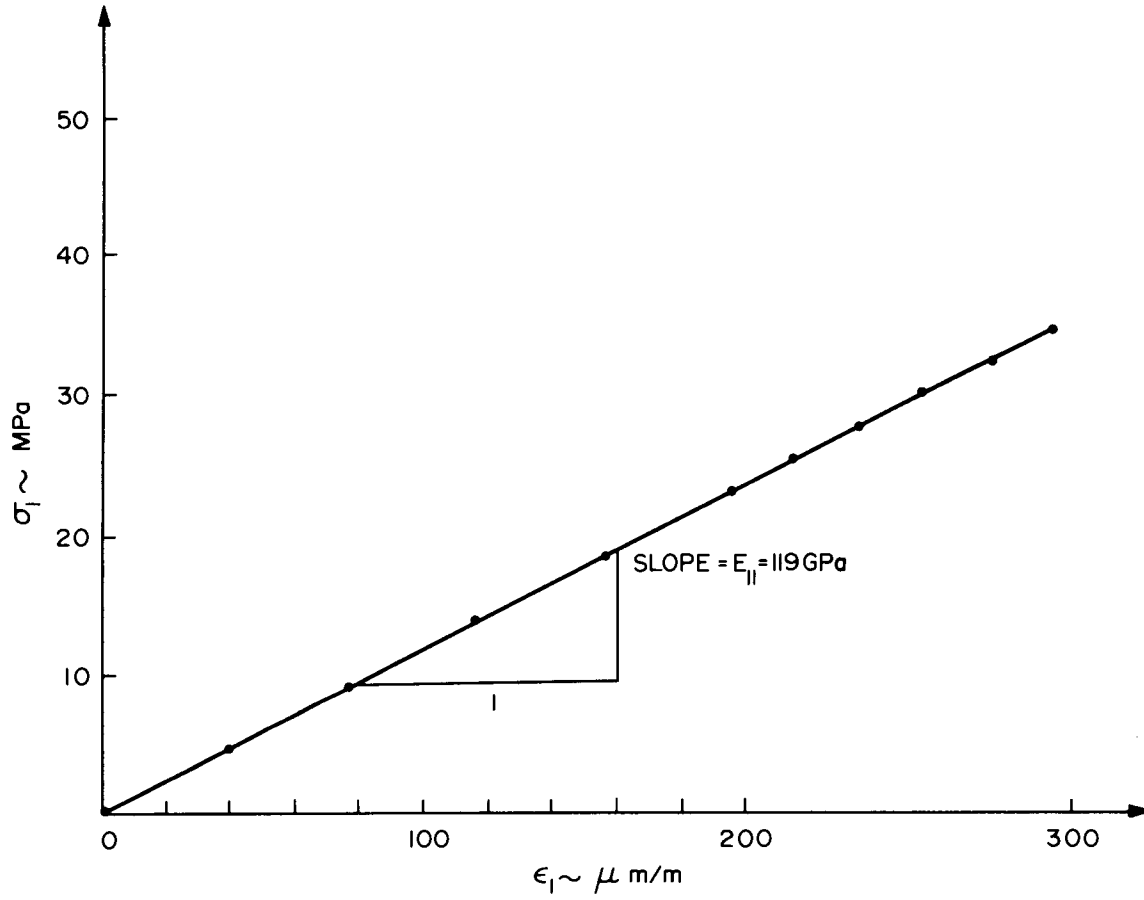


Figure 2

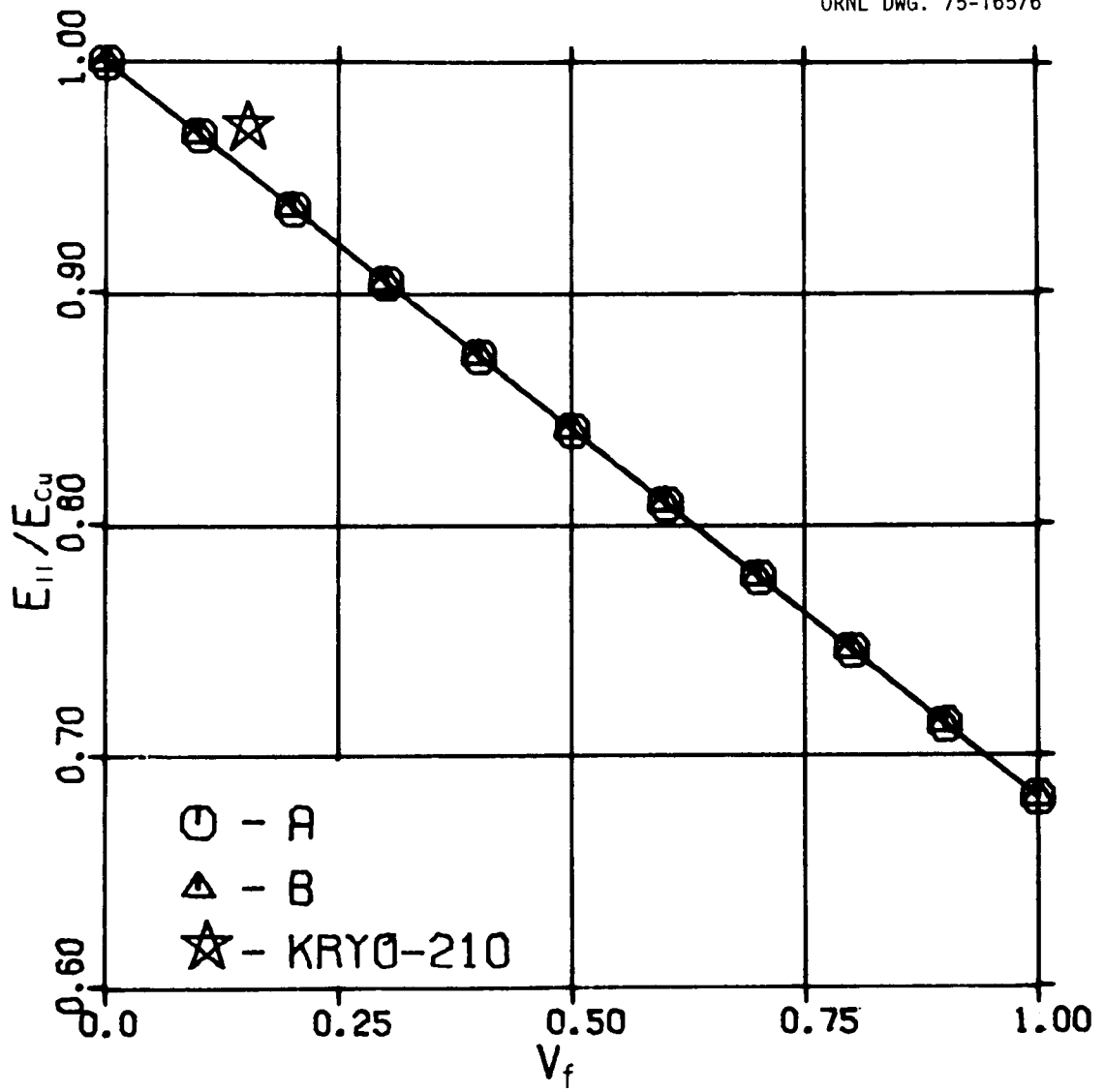


Figure 3

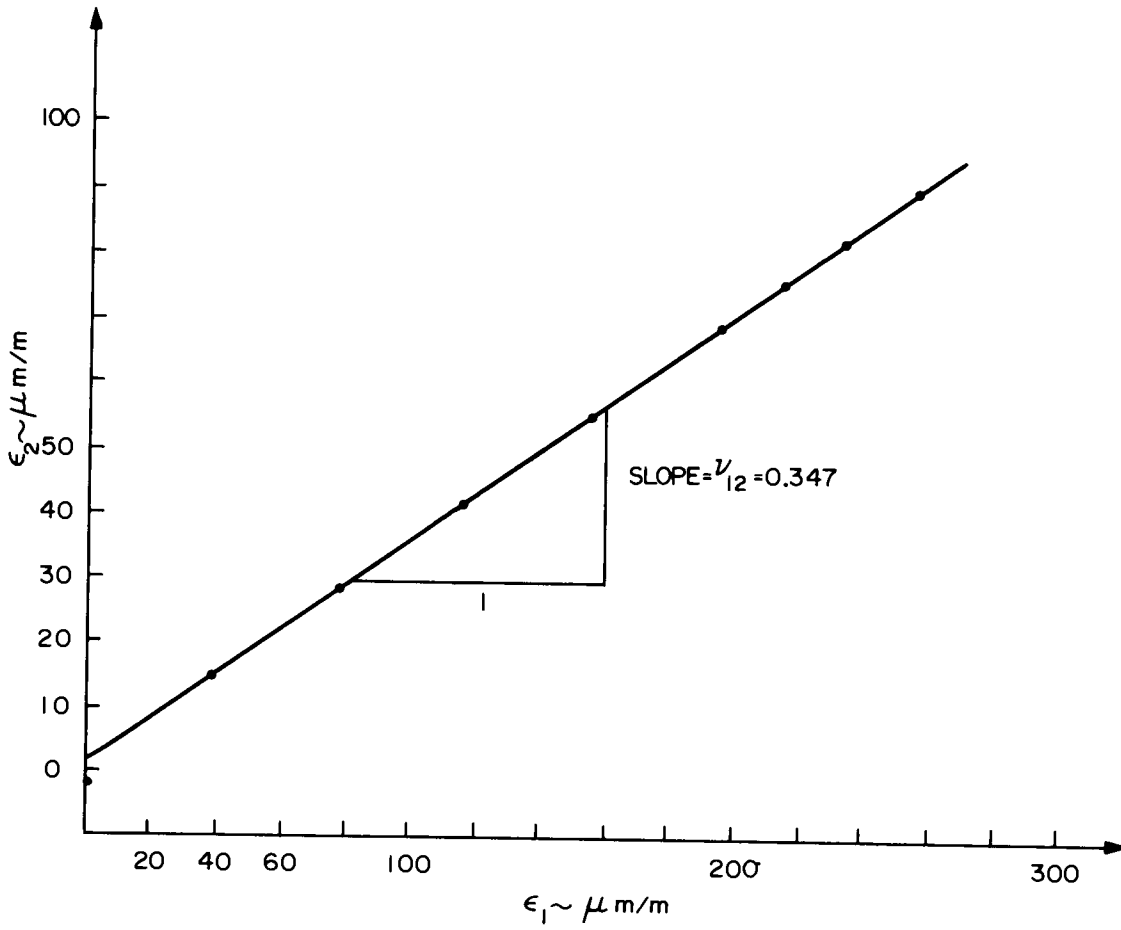


Figure 4

ORNL DWG. 75-16577

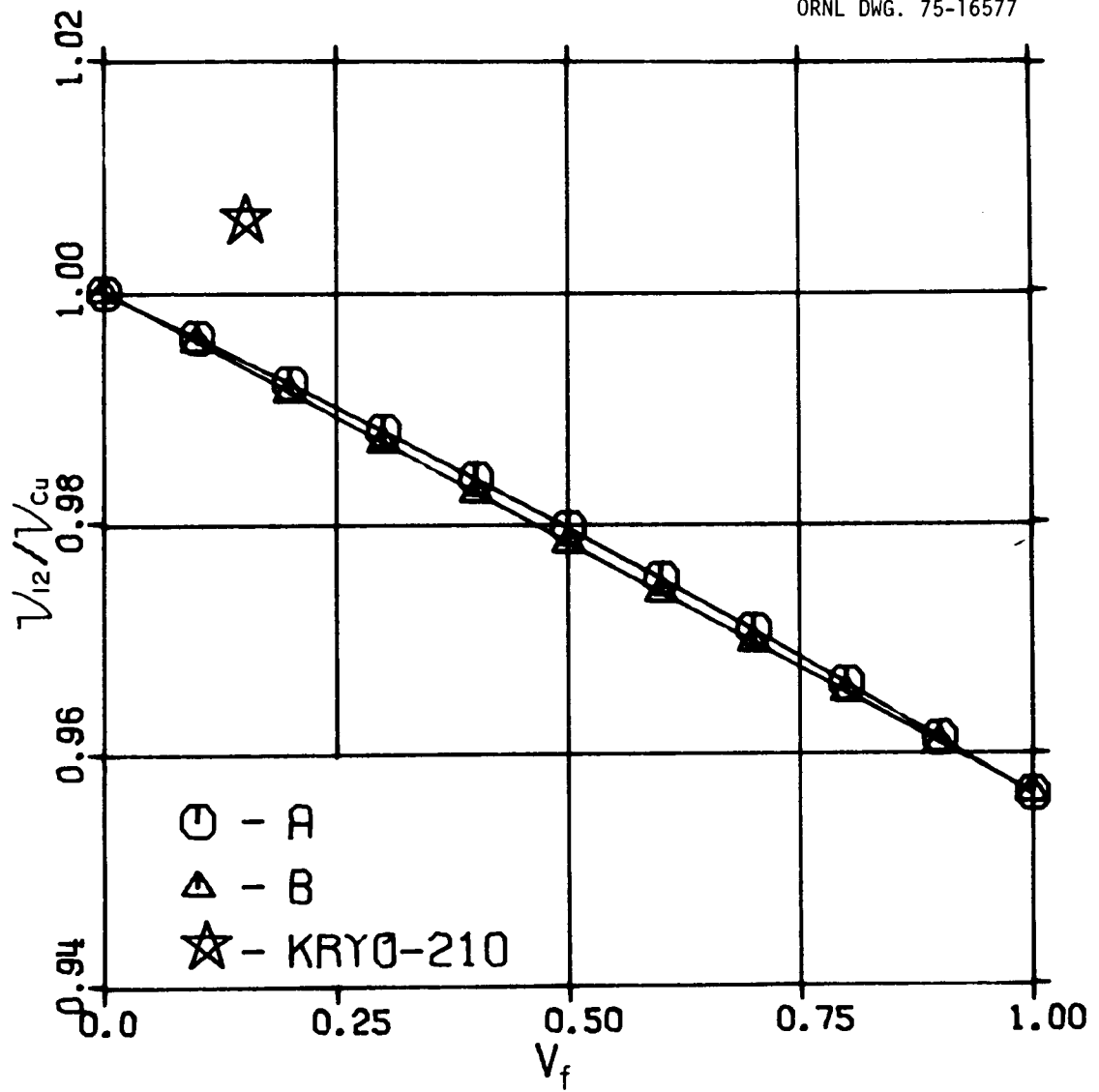


Figure 5

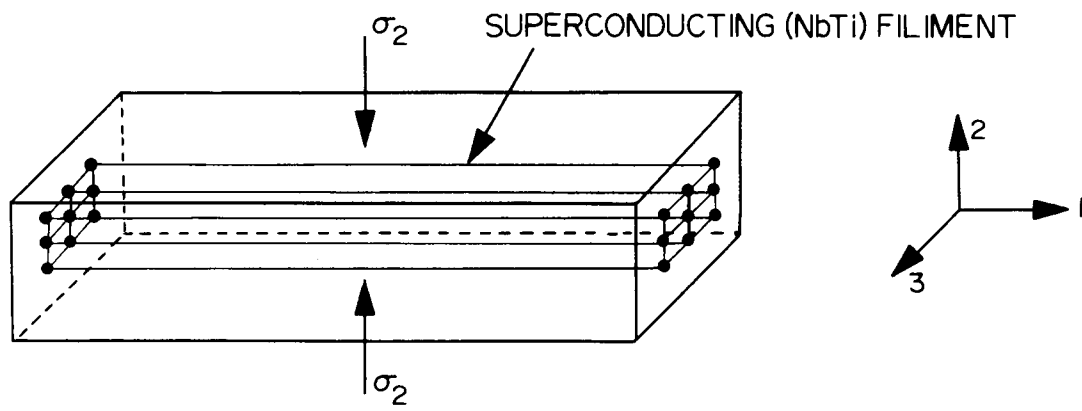


Figure 6

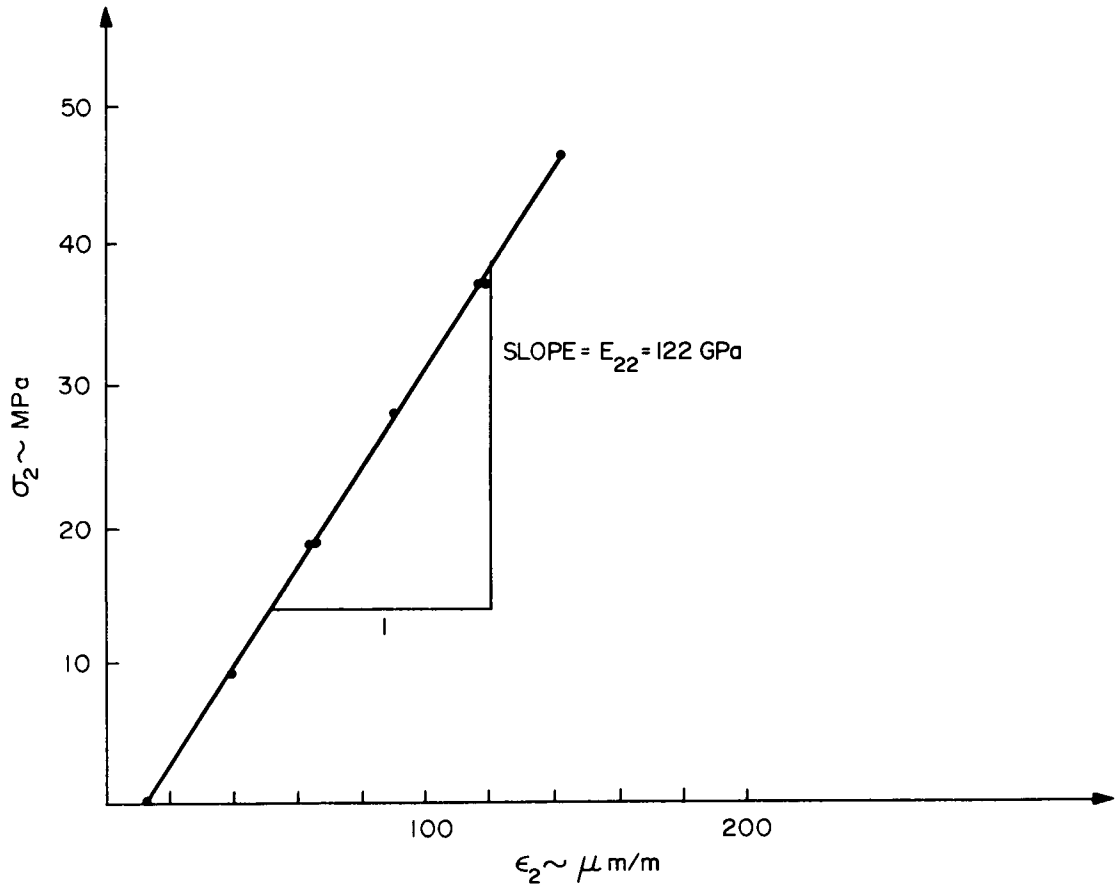


Figure 7

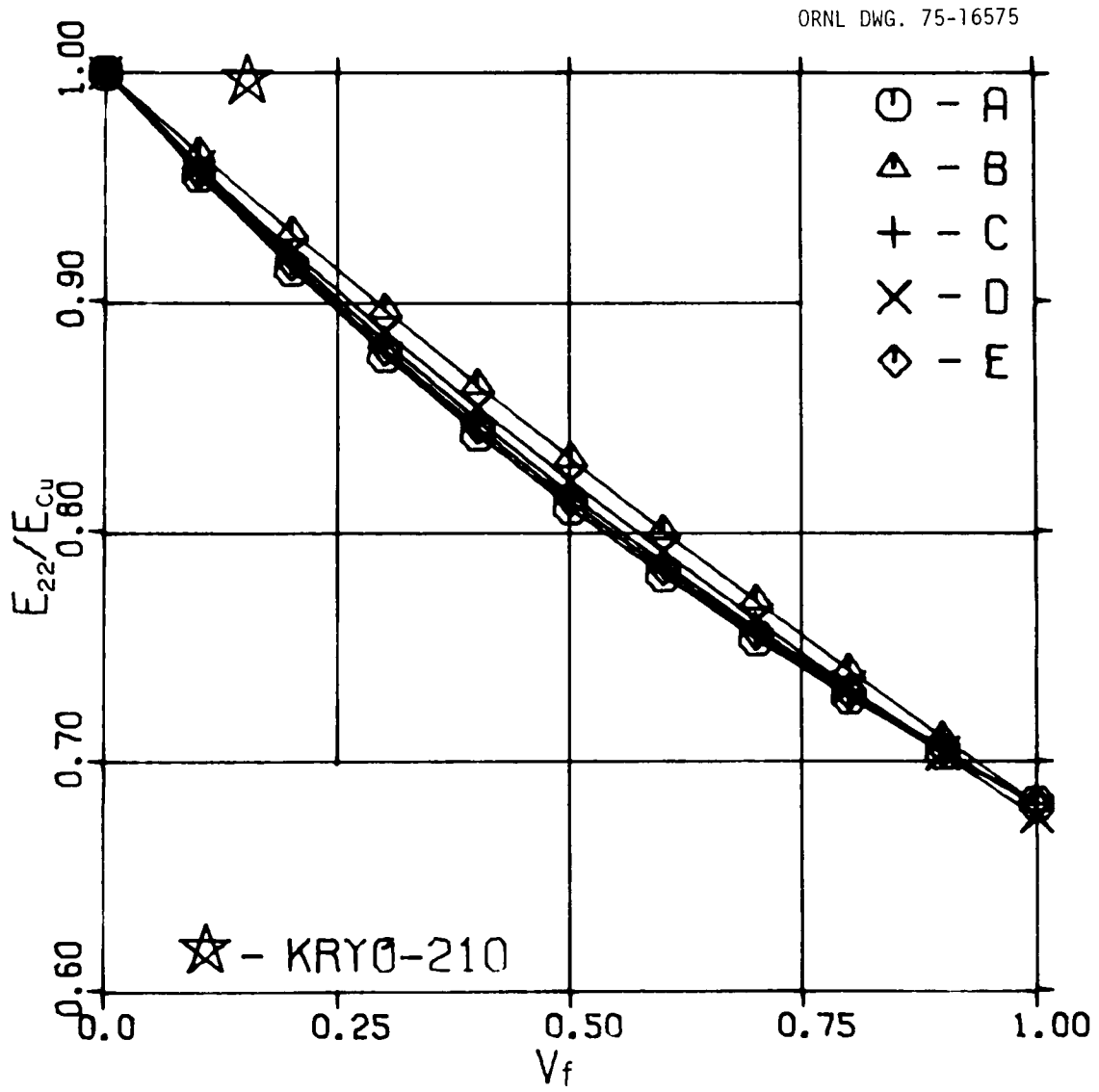


Figure 8

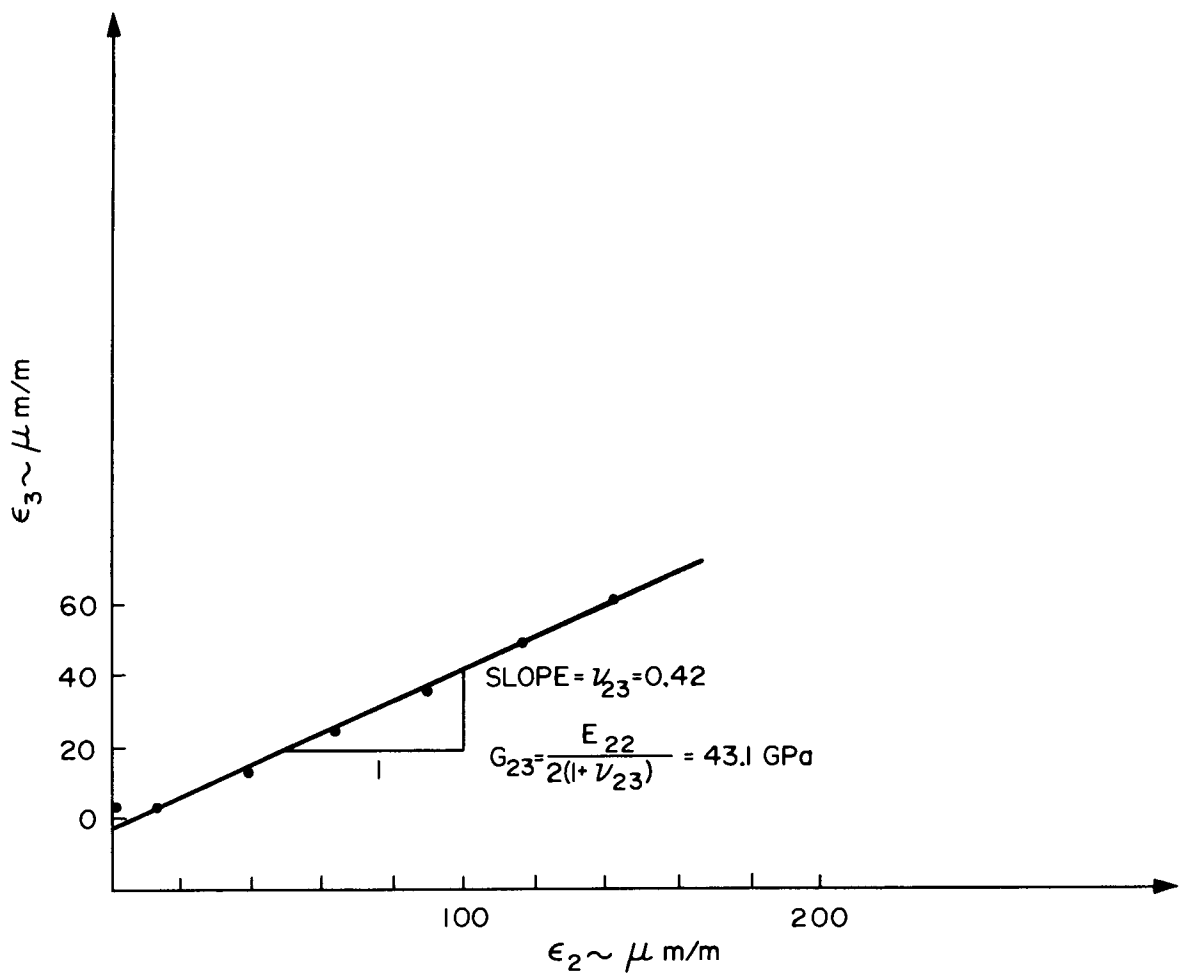


Figure 9

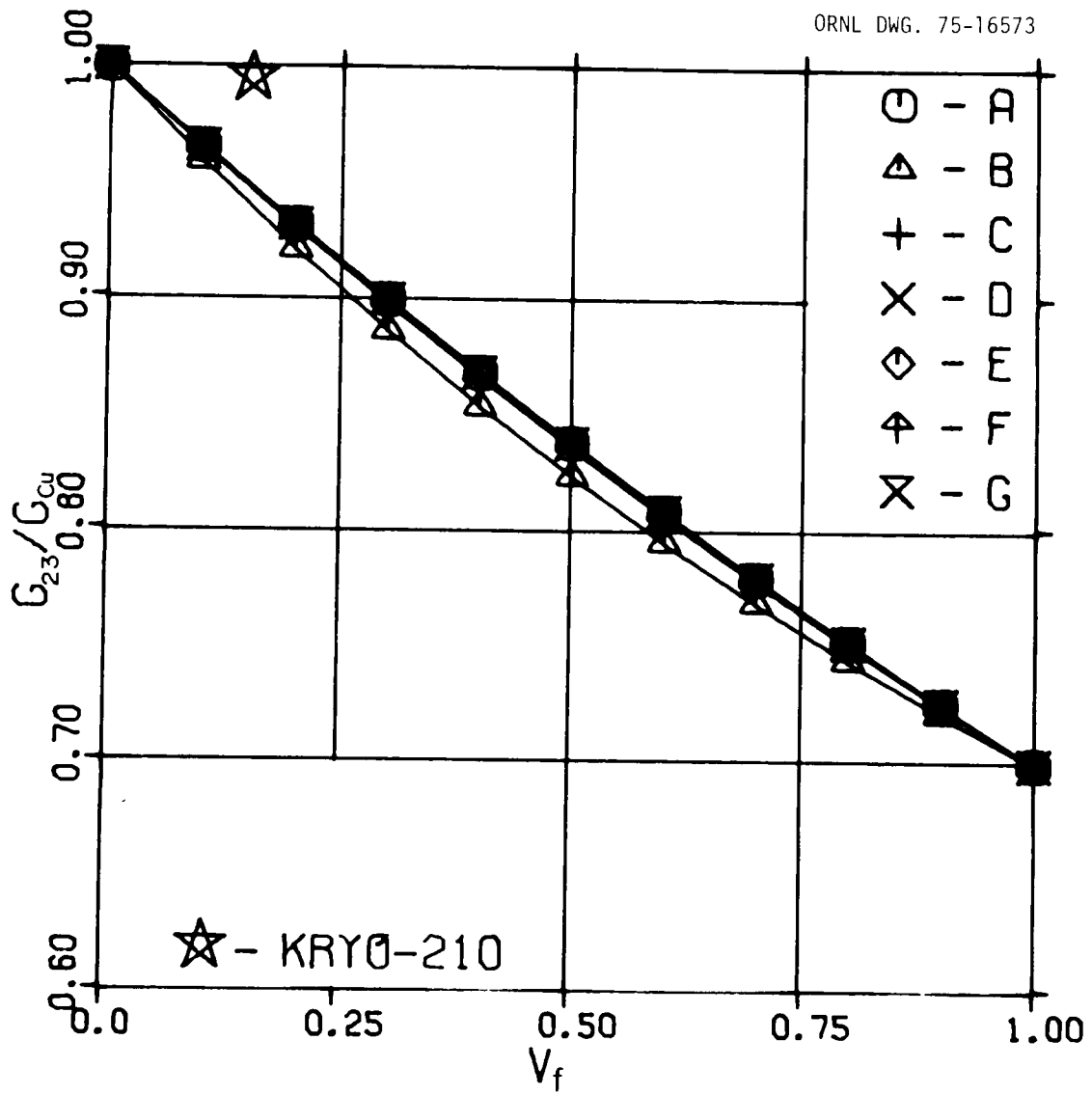


Figure 10

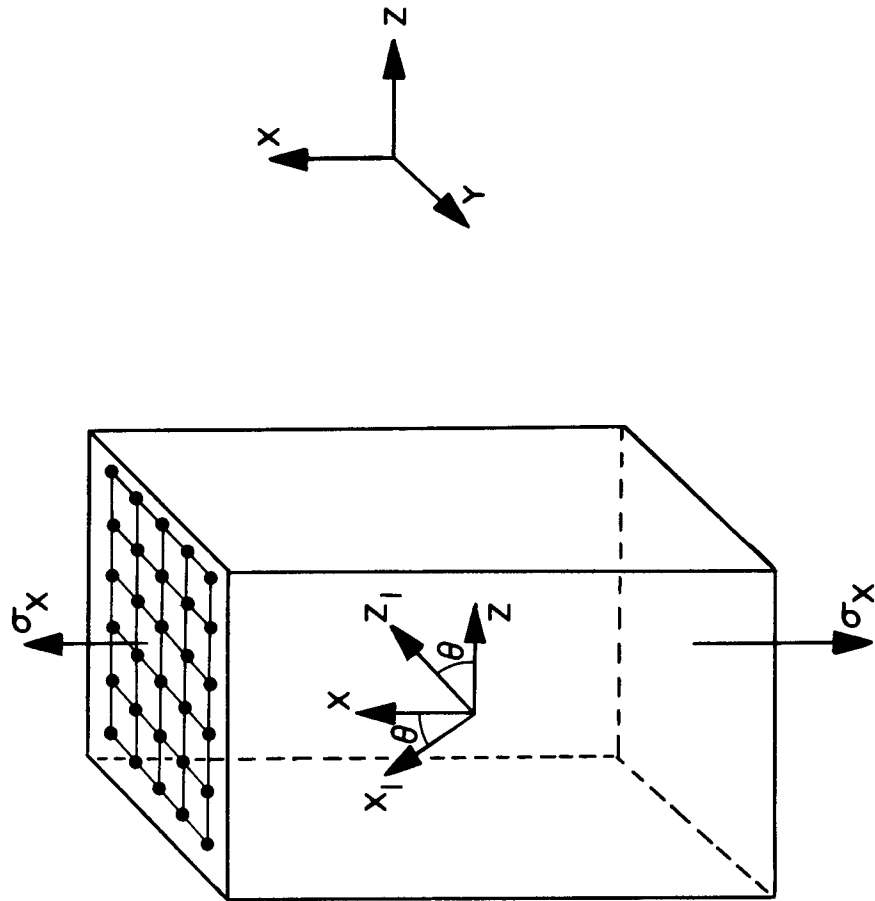


Figure 11

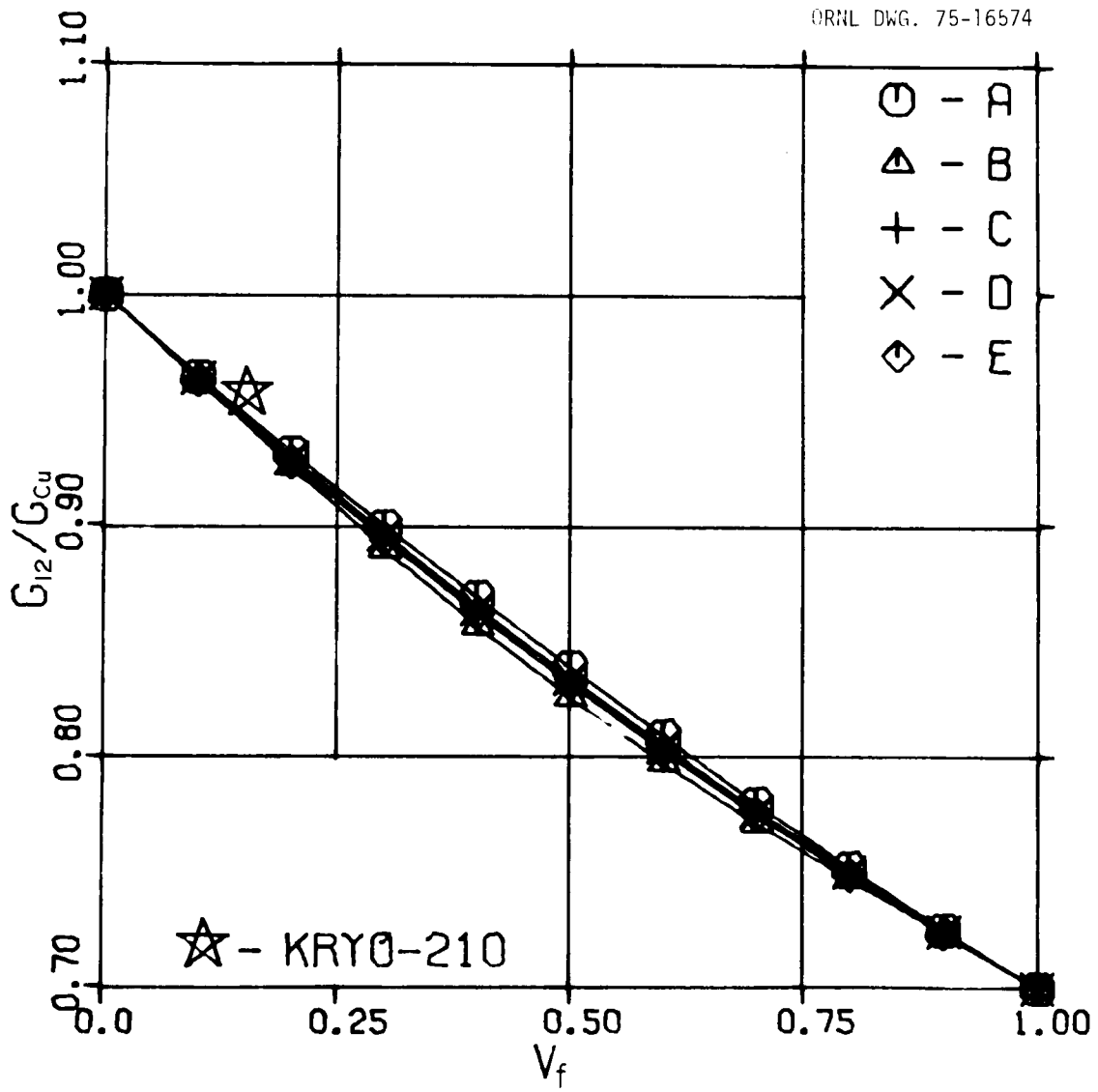


Figure 12

## INTERNAL DISTRIBUTION

- |        |                   |        |                         |
|--------|-------------------|--------|-------------------------|
| 1.     | W. C. Anderson    | 33.    | J. R. Miller            |
| 2.     | J. K. Ballou      | 34.    | O. B. Morgan            |
| 3.     | R. L. Brown       | 35.    | H. Pih                  |
| 4.     | E. H. Bryant      | 36.    | H. Postma               |
| 5.     | P. B. Burn        | 37.    | M. Roberts              |
| 6.     | W. D. Cain        | 38.    | M. W. Rosenthal         |
| 7.     | D. D. Cannon      | 39.    | R. E. Schwall           |
| 8.     | J. F. Clarke      | 40.    | T. E. Shannon           |
| 9.     | F. L. Culler      | 41.    | S. S. Shen              |
| 10.    | L. Dresner        | 42.    | J. E. Simpkins          |
| 11.    | J. F. Ellis       | 43.    | D. Steiner              |
| 12.    | W. A. Fietz       | 44.    | W. C. Stoddart          |
| 13.    | A. P. Fraas       | 45.    | P. B. Thompson          |
| 14.    | K. J. Froelich    | 46.    | P. L. Walstrom          |
| 15-22. | W. H. Gray        | 47.    | H. T. Yeh               |
| 23.    | P. N. Haubenreich | 48.    | A. Zucker               |
| 24.    | G. G. Kelley      | 49-50. | C. R. Library (2)       |
| 25.    | C. G. Lawson      | 51.    | CTR Reports Office      |
| 26.    | C. J. Long        | 52.    | Document Ref. Section   |
| 27.    | H. M. Long        | 53-54. | Lab Records Dept. (2)   |
| 28.    | J. K. Lovin       | 55.    | Lab Records, ORNL, R.C. |
| 29.    | M. S. Lubell      | 56.    | Patent Office           |
| 30.    | J. W. Lue         | 57-58. | Thermonuclear Division  |
| 31.    | J. N. Luton       |        | Library (2)             |
| 32.    | H. C. McCurdy     |        |                         |

## EXTERNAL DISTRIBUTION

59. E. Adam, Airco, 100 Mountain Avenue, Murray Hill, NJ 07974.
60. J. W. Beal, DCTR, ERDA, Mail Stop G-234, Washington, DC 20545.
61. R. W. Boom, 513 Engineering Research Building, University of Wisconsin, Madison, WI 53706.
62. D. L. Coffey, American Magnetics Inc., P.O. Box R, Oak Ridge, TN 37830
63. D. N. Cornish, Lawrence Livermore Laboratory, P.O. Box 808, Livermore, CA 94550.
64. M. D'Agostino, Grumman Aerospace Corp., Bethpage, NY 11714.
65. J. E. Darby, Jr., CTR Program, D208, Argonne National Laboratory, 9700 South Cass Avenue, Argonne, IL 60439.
66. R. W. Derby, 247 Third Street, Cambridge, MA 02141.
67. Director, Research & Technical Services Division, ERDA, Oak Ridge Operations, Oak Ridge, TN 37830.
68. R. W. Fast, Manager, Experimental Facilities, National Accelerator Laboratory, P.O. Box 500, Batavia, IL 60510.
69. J. J. Ferrante, General Electric Co., Schenectady, NY 12345.
70. J. File, Princeton University, Plasma Physics Laboratory, Princeton, NJ 08540.
71. W. S. Gilbert, Lawrence Berkeley Laboratory, University of California, Berkeley, CA 94120.

72. R. W. Gould, Dept. of Applied Physics, California Institute of Technology, Pasadena, CA 91109.
73. H. Grad, Courant Institute, New York University, 251 Mercer Street, New York, NY 10012.
74. E. Gregory, Airco, 100 Mountain Avenue, Murray Hill, NJ 07974.
75. W. V. Hassenzahl, Los Alamos Scientific Laboratory, P.O. Box 1663 Los Alamos, NM 87544.
76. C. D. Henning, DCTR, ERDA, Mail Stop G-234, Washington, DC 20545.
77. G. K. Hess, DCTR, ERDA, Mail Stop G-234, Washington, DC 20545.
78. C. K. Jones, Manager, Cryogenic Research Laboratory, Westinghouse Electric Corporation, R & D Center, Pittsburgh, PA 15235.
79. E. E. Kintner, DCTR, ERDA, Mail Stop G-234, Washington, DC 20545.
80. H. L. Laquer, Los Alamos Scientific Laboratory, P.O. Box 1663, Los Alamos, NM 87544.
81. C. Laverick, 543 Hampshire Lane, Boling Brook, IL 60439.
82. J. A. Mayhall, Lockheed, P.O. Box 1103, Huntsville, AL 35807.
83. D. B. Montgomery, MIT, National Magnet Laboratory, 170 Albany Street, Cambridge, MA 02139.
84. F. Moon, Dept. of Theoretical & Applied Mechanics, Cornell University, Ithaca, NY 14850.
85. R. W. Moses, Jr., University of Wisconsin, Madison, WI 53706.
86. J. R. Powell, Brookhaven National Laboratory, Upton, NY 11973.
87. J. R. Purcell, General Atomic Company, P.O. Box 81608, San Diego, CA 92138.
88. J. D. Rogers, Q-26, Los Alamos Scientific Laboratory, P.O. Box 1663, Los Alamos, NM 87544.
89. D. J. Rose, Dept. of Nuclear Engineering, Massachusetts Institute of Technology, Cambridge, MA 02139.
90. C. H. Rosner, Intermagnetics General Corp., Charles Industrial Park, New Karner Road, Guilderland, NY 12084.
91. W. B. Sampson, Brookhaven National Laboratory, Upton, Long Island, NY 11973.
92. Z.J.J. Stekly, Magnetic Corporation of America, 179 Bear Hill Road, Waltham, MA 02154.
93. B. P. Strauss, Fermi National Accelerator Laboratory, P.O. Box 500, Batavia, IL 60510.
- 94-120. TIC, Oak Ridge, TN 37830. (27)
121. C. E. Taylor, Lawrence Livermore Laboratory, P.O. Box 808, L-384 Livermore, CA 94551.
122. R. Thomas, General Atomic Company, P.O. Box 81608, San Diego, CA 92138.
123. S. T. Wang, Argonne National Laboratory, 9700 South Cass Avenue, Argonne, IL 60439.
124. J. M. Williams, DCTR, ERDA, Mail Stop G-234, Washington, DC 20545.
125. J. Wong, Supercon, Inc., 9 Erie Drive, Natick, MA 01760.
126. H. H. Woodson, Chairman, Dept. of Electrical Engineering, University of Texas at Austin, Austin, TX 78712.
127. E. J. Ziurys, Mail Stop G-234, DCTR, ERDA, Washington, DC 20545.